Interaction of Noncompetitive Inhibitors with an Immobilized α3β4 Nicotinic Acetylcholine Receptor Investigated by Affinity Chromatography, Quantitative−Structure Activity Relationship Analysis, and Molecular Docking

Krzysztof Jozwiak,[†,§] Sarangan Ravichandran,[‡] Jack R. Collins,[‡] and Irving W. Wainer*[,†]

Gerontology Research Center, National Institute on Aging, National Institutes of Health, 5600 Nathan Shock Drive, Baltimore, Maryland 21224, Advanced Biomedical Computing Center, National Cancer Institute−Frederick/SAIC, P.O. Box B, Building 430, Miller Drive, Frederick, Maryland 21702, and Medical University of Lublin, Staszica 6, 20-081 Lublin, Poland

Received March 24, 2004

A large number of drug substances act as noncompetitive inhibitors (NCIs) of the nicotinic acetylcholine receptor (nAChR) by blocking the ion flux through the channel. An affinity chromatography technique has been developed for investigating the interactions between NCIs and the α3β4 subtype of neuronal nAChR. The data obtained from the chromatographic study were used to construct QSAR models of the NCI−nAChR binding with both electronic and steric parameters observed as important descriptors. A molecular model of the transmembrane domain of the α3β4 subtype of nAChR was constructed and used to simulate the docking of a series of NCIs. A key aspect of the model was the discovery of the cleft produced by the incorporation of the bulky phenylalanine moiety into the nonpolar section of the lumen by the β4 subunit. Quantitatively, the results of docking simulations modeled the experimental affinity data better than QSAR results. The computational approach, combined with the modeling of NCI−nAChR interaction by affinity chromatography, can be used to predict possible toxicities and adverse interactions.

1. Introduction

Neuronal nicotinic acetylcholine receptors (nAChRs) are a family of ligand gated ion channels found in the central and peripheral nervous systems that regulate synaptic activity.[1,2] nAChRs are a key target in drug discovery for a number of diseases, including Alzheimer's and Parkinson's disease, and have been widely discussed and investigated.[3−5]

The nAChR is formed by bringing together five separate transmembrane proteins (subunits), each containing a large extracellular N-terminal domain, four membrane-spanning α helices (M1, M2, M3, and M4), and a small C-terminal domain[2] (see Figure 1). The subunits are oriented around a central pore,[4,6] and the resulting transmembrane ion channel is formed by a pentameric arrangement of the M2 helical segments contributed by each of the five proteins[7] (see Figure 1).

At present, 12 different neuronal subunits have been identified, nine labeled α (α2−α10) and three labeled β (β2−β4). The subunits form channels of a wide variety of homomeric and heteromeric neuronal nAChRs.[8] The most common subunit stoichiometry has been determined to be $(\alpha X)_2(\beta Y)_3$ ($X = 2-4$; $Y = 2-4$) for heteromeric subtypes and $(\alpha Z)_5$ ($Z = 7-10$) for the homomeric subtypes.[9] However, other more complex combinations have also been reported.[10]

nAChR subtypes are found in different locations of the central and peripheral nervous system and have been assigned different pharmacological functions, For instance, the α4β2 and α4β4 subtypes appear to play a role in cognition, neurodegeneration, pain, anxiety, and depression; the α3β2 subtype plays a role in dopamine release and Parkinson's disease; the α7 plays a role in GABA release; the α9 plays a role in auditory function and development; and the α3β4 plays a role in norepinephrine release and cardiovascular and gastrointestinal action.[10]

The nAChR contains multiple binding domains that can accommodate different classes of endogenous and exogenous compounds.[5] Two homologous neurotransmitter binding sites are formed by the N-terminal domains where agonists and competitive antagonists bind. This site has been the subject of a number of structure−activity relationship (SAR) studies (cf. refs 11−13) because of its recognized therapeutic importance and because of the availability of rapid and facile experimental procedures to determine binding and functional properties.

The nAChR contains several other binding sites at which noncompetitive inhibitors (NCIs) may bind.[5,14] A key binding site is the luminal high-affinity NCI binding domain, which is located on the surface of the internal lumen that forms the ion channel. The ends of the internal lumen of the nAChR are highly polar and negatively charged. This domain can be viewed as a cation selector in which NCIs bearing a positive charge, usually on an amine moiety, are trapped and directed down the channel by an electrostatic gradient.[15] The NCIs then bind at a site at the narrowest region of the channel, which essentially plugs the channel and blocks ion flux.[14] This mechanism has been used to describe the noncompetitive inhibitory properties of drugs such as mecamylamine and dextromethorphan,[16] bupropion and phencyclidine,[17] and barbiturates.[18]

* To whom correspondence should be addressed. Phone: 410-558-8498. Fax: 410-558-8409. E-mail: wainerir@grc.nia.nih.gov.
† National Institute on Aging.
§ University of Lublin.
‡ National Cancer Institutes−Frederick/SAIC.

10.1021/jm0400707 CCC: $27.50
Published on Web 06/29/2004

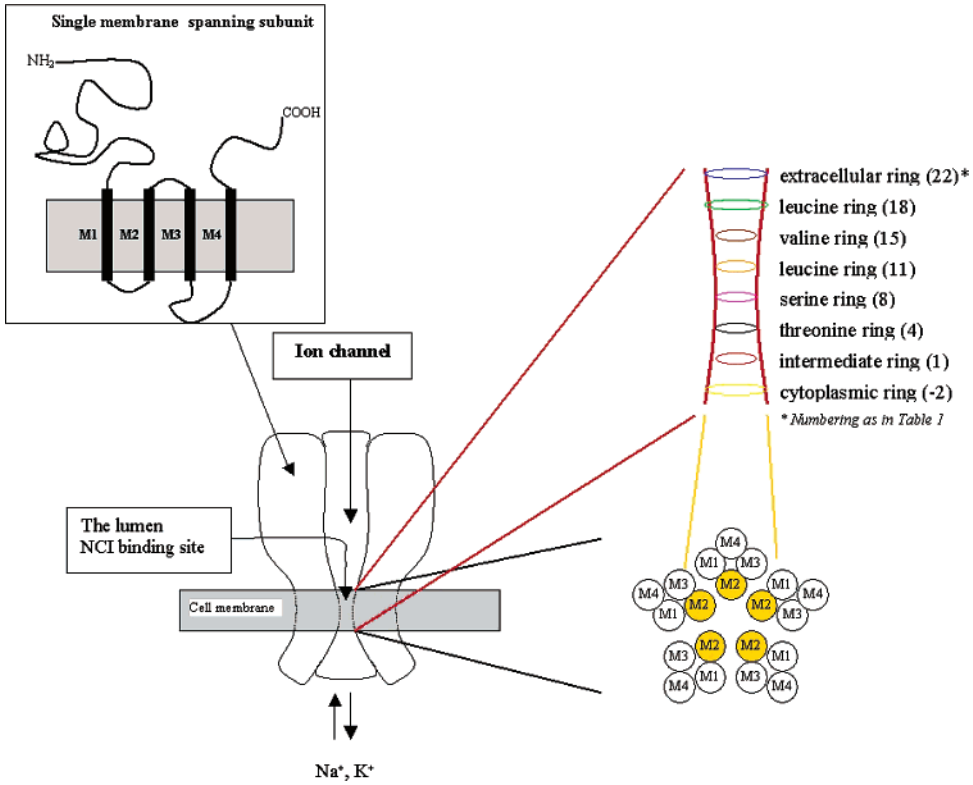

Figure 1. Schematic representation of the nicotinic acetylcholine receptor showing the relationship of the receptor to the ion channel, the membrane, and the arrangement of the four transmembrane-spanning helices forming the channel. The various regions of the channel "rings" are also shown (adapted from refs 2 and 5).

A number of marketed drugs and their metabolites[16,17,19−23] have been identified as NCIs of nAChRs, and this property may be responsible for many of the side effects attributed to these compounds. For example, the impairment of cardiovascular function observed during ketamine anesthesia has been associated with the inhibitory action of ketamine on ganglionic nAChRs[24] and the constipation associated with the administration of mecamylamine and methadone may also be associated with their noncompetitive inhibition of the α3β4 nAChR. NCIs also present an opportunity for new drug development. The antidepressants sertraline, paroxetine, nefazodone, and venlafaxine have been identified as potent NCIs, and it has been suggested that nAChR subtypes in the brain could be targets for the development of new antidepressant drugs.[21] The NCIs mecamylamine and bupropion are currently used in antismoking therapy,[25] and the use of the NCI 18-methoxycoronaridine in combination with mecamylamine or dextromethorphan has been suggested as an approach for the treatment of opioid and stimulant addiction.[26]

Thus, the determination of a compound's activity as an NCI of the nAChR could be a key to the preclinical detection of drug toxicities, e.g., ketamine, or the development of a new class of therapeutic agents. However, the identification of a compound as an NCI is time-consuming and exacting. This determination has been primarily accomplished using functional studies involving nicotine-stimulated $^{86}Rb^{+}$ efflux assays[16] or electrophysiological approaches.[24]

We have recently reported an alternative approach to the study of ligand interactions with the nAChR, which is based on frontal and nonlinear affinity chromatography on an immobilized α3β4 nAChR stationary phase.[27,28] The immobilized nAChR column can be used to characterize both agonists and NCIs and can be continuously used for several months. Displacement chromatographic studies have also demonstrated that agonists can be differentiated from NCIs; i.e., the addition of an agonist to the mobile phase will reduce the retention of an agonist but not an NCI and vice versa.[28]

The frontal affinity chromatography technique has been used in the rapid determination of the affinity of agonists and competitive antagonists. The nonlinear approach has been used to identify and characterize NCIs, including the thermodynamics and kinetics of the NCI−nAChR interactions and the determination of enantioselective interactions.[29] In the latter case, it was observed in the chromatographic experiments that dextromethorphan exhibited a higher affinity to the α3β4 nAChR column than its enantiomer levomethorphan. This difference was primarily due to the longer dissociation time for the dextromethorphan−receptor complex (k_{off} = 1.01 vs 1.55 s^{-1} for levomethorphan), and subsequent analysis suggested that it was an enthalpic effect.[29] This effect was further observed and confirmed by functional studies in a cell line expressing α3β4 nAChR, where the duration of the receptor inhibition in nicotine-stimulated $^{86}Rb^{+}$ efflux experiments was significantly longer for dextromethorphan than for levomethorphan.[29]

The initial studies of the characterization of NCIs on an immobilized α3β4 nAChR column utilized only four compounds.[28] In the present work, 25 compounds, 20 NCIs, and 5 controls (Figure 2) were studied in order to further characterize the interactions between NCIs and the immobilized nAChR stationary phase. The

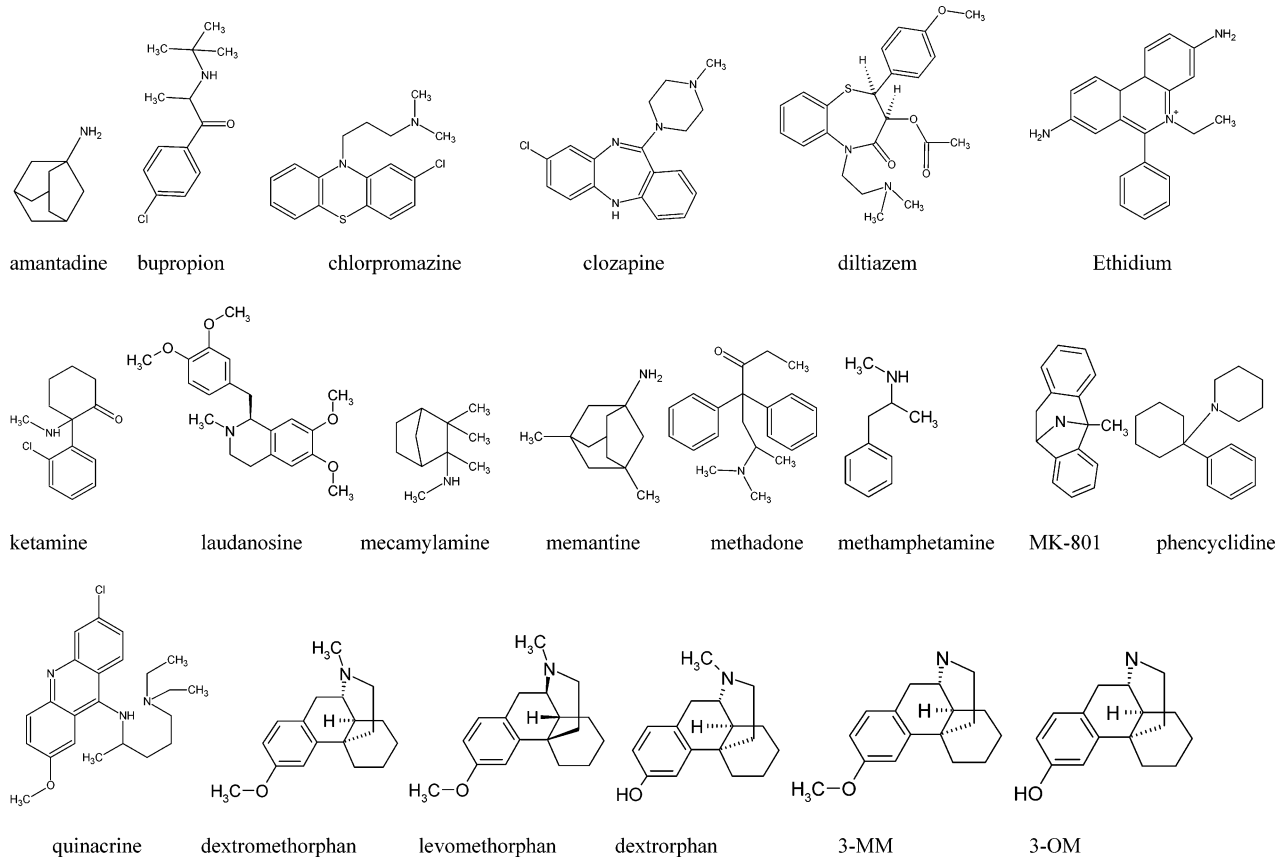

Figure 2. Chemical formulas of tested NCIs.

Table 1. Sequence Alignment of M2 Transmembrane Section across Different Subunits of nAChRs[a]

	1	2	3	4	5	6	7	8	9	10	11	12	13	14	15	16	17	18	19	20	21	22	23
alpha 3	E	K	V	T	L	C	I	S	V	L	L	S	L	T	V	F	L	L	V	I	T	E	T
alpha 4	E	K	I	T	L	C	I	S	V	L	L	S	L	T	V	F	L	L	L	I	T	E	I
alpha 5	E	K	I	C	L	C	T	S	V	L	V	S	L	T	V	F	L	L	V	I	E	E	I
alpha 6	E	K	V	T	L	C	I	S	V	L	L	S	L	T	V	F	L	L	V	I	T	E	T
alpha 7	E	K	I	S	L	G	I	T	V	L	L	S	L	T	V	F	M	L	L	V	A	E	I
alpha 9	E	K	V	S	L	G	V	T	I	L	L	A	M	T	V	F	Q	L	M	V	A	E	I
alpha 10	E	K	V	S	L	G	V	T	V	L	L	A	L	T	V	F	Q	L	L	V	A	E	S
beta 2	E	K	M	T	L	C	I	S	V	L	L	A	L	T	V	F	L	L	L	I	S	K	I
beta 3	E	K	L	S	L	S	T	S	V	L	V	S	L	T	V	F	L	L	V	I	E	E	I
beta 4	E	K	M	T	L	C	I	S	V	L	L	A	L	T	F	F	L	L	L	I	S	K	I

[a] Source is the ENTREZ Protein Databank at the U.S. National Library of Medicine. Residues on yellow background are exposed to the center of the channel and form rings (colored as rings in Figure 1).

chromatographic data were used to build conventional QSAR models to describe and predict these interactions. However, the enantioselective interaction between dextromethorphan and levomethorphan could not be described by a 2D QSAR approach; i.e., the QSAR models did not contain descriptors reflecting the enantioselective interactions. To address this question, a molecular model of the transmembrane $\alpha 3\beta 4$ nAChR luminal domain has been built and a series of in silico docking studies were performed.

The molecular target of this study is the pentameric bundle of M2 helices forming the "lumen" (Figure 1), the central surface of the narrowest part of the channel, which takes part in channel gating and ion selection. Previous studies have demonstrated that the M2 helices are oriented in a 5-fold symmetrical manner, that the amino acid residues forming the surface of the lumen are fundamentally conserved across different subunits, and that they form distinct regions of the channel, or "rings" (see Figure 1 and Table 1).[14] These rings are important for proper function and selectivity of the neuronal nAChRs and are common to all subtypes.[7] An illustration of this importance is the fact that even a single point mutation in this domain can lead to a

variety of serious diseases, e.g., autosomal dominant nocturnal frontal lobe epilepsy, associated with a single point mutation in the M2 segment of the α4 subunit of nAChR.[30] Therefore, the sequence and structure of the M2 subunits forming the luminal domain are of critical importance for understanding disease states associated with nAChRs.

Several previous studies have proposed molecular models of the transmembrane domains of neuronal nAChRs. Sansom and co-workers explored the bundle of five M2 helices of the α7 nAChR subtype,[31,32] and Barrantes and co-workers presented models of the whole transmembrane domain containing all 20 segments of α7 nAChR.[33,34] Miyazawa and co-workers, using cryo-electron microscopy images, have recently developed models of the *Torpedo marmorata* nAChR ($\alpha\beta\delta\gamma$).[35] These publications have mainly focused on the structural and functional issues and have explored the differences between open and closed states and the cation selection mechanism. However, they have not addressed subtype-specific issues of neuronal nAChRs or interaction with actual and potential NCIs.

Other publications have more directly addressed the issue of ligand interaction with nAChR channels. One study examined the complex formed by pentobarbital and a model of the open α7 nAChR,[18] and the results demonstrated that pentobarbital was primarily bound to a hydrophobic environment near the valine (V) ring (position 15, Table 1) of the nAChR. In another study, Ortells and Barrantes[36] performed a series of docking simulations between a number of ligands and the luminal region of the α7 nAChR to help clarify experimental data derived from photoaffinity labeling, site directed mutagenesis, and binding data. The docking studies revealed that the ligands mainly bound to the region of the channel near the serine (S) and threonine (T) rings at positions 4 and 8, respectively, with minor interactions also observed at positions 1, 12, and 15 of the lumen.[36] These studies suggest that these ligands, and possibly others, bind to specific regions in the lumen.

While the general structure of the luminal domain is fairly well conserved among the neuronal subtypes of the nAChRs, specific subtypes may have particular properties that change the selectivities and the interaction mechanisms. Of particular interest is position 15, at which most of the subunits have a valine moiety except for the β4 subunit, which has a phenylalanine (F)[37] (Table 1). It is generally accepted that residues at position 15 are exposed to the center of the channel, forming one of the rings and playing a role in channel gating.[37] Therefore, nAChRs containing the β4 subunit should be expected to display significantly different properties than other subunit types, which could affect the interaction of the nAChR channel with NCIs.

In this work, the molecular model of the α3β4 nAChR luminal domain was created and used to dock the compounds from the chromatographic portion of the study with special attention being paid to the explanation of the enantioselective interaction between dextromethorphan and levomethorphan. The results of the docking studies were compared and correlated with the experimental data from affinity chromatography. The QSAR and docking models may be useful in the prediction of the drug side effects due to noncompetitive binding at these receptors and as a tool in new drug discovery. The chromatographic and docking approaches can be easily extended to test other subtypes of neuronal nAChRs in order to study subtype-specific drug interaction.

2. Methods

2.1. Nonlinear Affinity Chromatography. A detailed description of nonlinear chromatography on an α3β4 nAChR affinity column and its application in the investigation of known NCIs of the nAChR has been previously reported.[28] Briefly, a chromatographic column containing a stationary phase with an immobilized protein has typically a limited (and relatively low) number of active binding sites. A known concentration of tested ligand is injected into the column, and the migration of the ligand through the column produces a skewed peak with reduced centroids instead of regular Gaussian shapes. The broadness and asymmetry of the peak profile is a product of the actual kinetics of association and dissociation of the ligand−immobilized protein complexes, which are not infinitely fast.[38] By use of a nonlinear isotherm, the distorted peak profile can be described as a mathematical function of applied concentration and the kinetics of ligand−immobilized protein interactions occurring during the chromatographic process.[39] In our previous studies we employed the mathematical function called the impulse input solution developed by Wade et al.[40] to fit to experimental peak profiles obtained in nAChR columns.[28,29] The fitting procedure produces four variable parameters, which can be further used to calculate four descriptors of the affinity chromatography process:

1. k', real thermodynamic capacity factor,
2. k_{off}, solute desorption rate constant,
3. k_{on}, solute adsorption rate constant,
4. K, equilibrium constant for adsorption ($K = k_{on}/k_{off}$).

The use and the range of the application of the nonlinear chromatography approach in the study of the interaction between NCIs and the α3β4 nAChR column have been validated and discussed in previous reports.[28,29] The results of these studies demonstrated that the approach could be employed to rapidly determine if a compound acts as an NCI and to characterize its affinity toward the immobilized receptor. In addition, if other compounds are chromatographed using the same experimental conditions, the relevant chromatographic parameters can be calculated from a single chromatographic experiment with the average standard error of determination for k', k_{off}, k_{on}, and K values being estimated as 0.25 s^{-1}, 0.01 s^{-1}, 1 μM^{-1} s^{-1}, and 0.3 μM^{-1}, respectively. This produces a rapid method that can assess the relative binding of a series of compounds. On average, the analysis of a single compound takes 2 h and the single column can be continuously used for several months.

The impulse input solution equation was implemented in a commercially available software for chromatographic signal deconvolution[41] and can be used for nonlinear processing of the chromatographic profiles.

2.2. QSAR Models. Various structural descriptors were calculated for tested neutral compounds using the

QSAR+ module of Cerius2, version 4.8,[42] and the QSAR Properties module of HyperChem, version 6.0.[43] STATISTICA, version 6.0,[44] was used for regression and the development of the QSAR models. The stepwise multiple linear regression technique was used to generate the QSAR models.

2.3. α3*β*4 nAChR Channel Model. It has been previously reported that a synthetic 23-mer peptide, homologous to the sequence of the putative transmembrane M2 segment of the *Torpedo californica δ* nAChR subunit, spontaneously forms discrete ion channels in liposome bilayers.[45] These channels are functionally similar to the nAChR channel when properties such as single-channel conductances, discrimination of cations over anions, and channel lifetimes for open and closed states are compared.[45,46] In addition, these channels were found to be blocked by certain NCIs, as are the native channels.[47] By use of frozen-state NMR techniques, the structure (Protein Data Bank code = 1EQ8) was shown to consist of five α-helical polypeptides oriented in a 5-fold symmetrical manner forming a funnel-like architecture with a wide opening on the N-terminal side and preserving the sequence of "rings" along the channel as in natural nAChRs[48] (see Figure 1). In light of the similarities between the synthetic model and biological nAChR channels, we used this model as a starting point for exploring the mechanism of inhibition of the receptor by luminal NCIs presented here.

We initially modified the PDB entry 1EQ8 by mutating the *δ* M2 residues into α3 and *β*4 sequences (Table 1) using SYBYL 6.8.[49] This resulted in a heteropentameric channel with α3, *β*4, α3, *β*4, and *β*4 helices, respectively. The model was further refined by energy minimization using the Sander_Classic module of Amber 6.0.[50] The termini of each helix were blocked in the standard AMBER procedure by adding acetyl beginning groups (ACE) and *N*-methylamine ending groups (NME). The AMBER'94 force field[51] parameters were used for energy minimization with a convergence criterion of the root mean square of the gradient being less than 1.0×10^{-4} kcal mol^{-1} Å^{-1}. Each minimization run was started with the steepest descent followed by the conjugate gradient method, and a distance-dependent dielectric function was used to evaluate the electrostatic energy. Energy minimizations were performed in stages by relaxing (i) only hydrogen atoms, (ii) hydrogen + side chain atoms, and (iii) all atoms except α carbons. Finally, a restrained minimization on the α carbons of the model was also performed. This was done to relax the model while keeping its overall orientation similar to the template structure. The final model of the α3*β*4 nAChR luminal domain was evaluated using Procheck.[52]

The final model of the α3*β*4 nAChR luminal domain is depicted in Figure 3. Figure 3a shows the stereoview of the five α helices forming the channel and their alignment relative to each other. Figure 3b illustrates the location of the specific amino acid rings distributed along the channel. The internal luminal surface has ionized residues on both ends of each helix, which appear to be responsible for ion selection of the nAChRs. Seven rings of amino acids are clearly visible along the channel in Figure 3b. An extracellular polar ring (E/K) at the edge of the membrane is followed in sequence by three nonpolar (L, V/F, and L) and then three polar (S, T, and intermediate (E)) rings. The cytoplasmic ring of acidic residues (see Figure 1) was not included in our model. Since the α3*β*4 nAChR subtype is a heteropentamer composed of two different subunits, one of the rings (position 15 in Table 1) is formed by two different residues. This important feature of the α3*β*4 channel introduces phenylalanine in position 15 (V/F ring). This polymorphism results in the formation of asymmetric hydrophobic clefts between the α3 and the *β*4 helices at the interface between the isopropyl and phenyl moieties associated with V and F, respectively. This particular feature would not exist in non-*β*4 subtypes, which would only possess V residues at this site (see Table 1).

The final model of the luminal domain of the α3*β*4 nAChR was compared with the recently reported model of the transmembrane segment of α*βδγ* nAChR (PDB code = 1OED).[35] The overall orientations and positions of the channel helices are quite similar except for some minor heterogeneity due to the different subunit compositions and residue-specific interactions inside the lumen. Thus, the features of our model appear consistent with the latest experimental data.

The coordinates of the α3*β*4 nAChR channel model are presented in Supporting Information.

2.4. Ligand Structures. The molecular structures of the NCI ligands used in the docking simulations (Figure 2) were built in HyperChem.[43] Both the ionized and neutral states of each NCI were used in the simulations. We also included five other structures, known to not be NCIs, in their neutral ionization states, which were docked as negative controls. Thus, a total of 39 molecular ligands were built (17 protonated NCIs, 17 neutral NCIs, and 5 neutral controls). The AM1 semiempirical method[53] was used to minimize the ligand energy and to calculate partial atomic charges. Partial atomic charges of each tested ligand are provided in Supporting Information. Atomic coordinate files were converted into AutoDock.pdbq files using the HIN2PDBQ script [Johansson, M. Some Computational Chemistry Related Python Conversion Scripts (2002); http://www.helsinki.fi/%7Empjohans/python].

2.5. Docking Simulations. AutoDock-3.0.5[54] was used to study the binding of ligands to the model of the luminal domain of α3*β*4 nAChR. AutoDock is composed of three programs: AutoTors, AutoGrid, and AutoDock. The algorithms are described in detail elsewhere.[54,55] AutoDock keeps the target protein structure rigid while ligands are conformationally flexible during docking. The AutoTors module reads in the inhibitor and identifies the torsionally flexible and rigid bonds in the molecule. The AutoGrid module precomputes the atomic affinity potential grids using specific atomic probes for each atom type in the inhibitor and stores them in the form of maps. In our computations, a grid composed of $60 \times 60 \times 120$ points (22.5 Å × 22.5 Å × 45 Å box) with a grid spacing of 0.375 Å was used. This grid completely covered the binding area of the lumen. A dielectric constant of 15 was used for constructing the electronic grid maps based on a series of test runs (explained in detail in the Supporting Information). Finally, AutoDock was used to perform the docking simulations, with the interaction energies calculated using the AMBER force

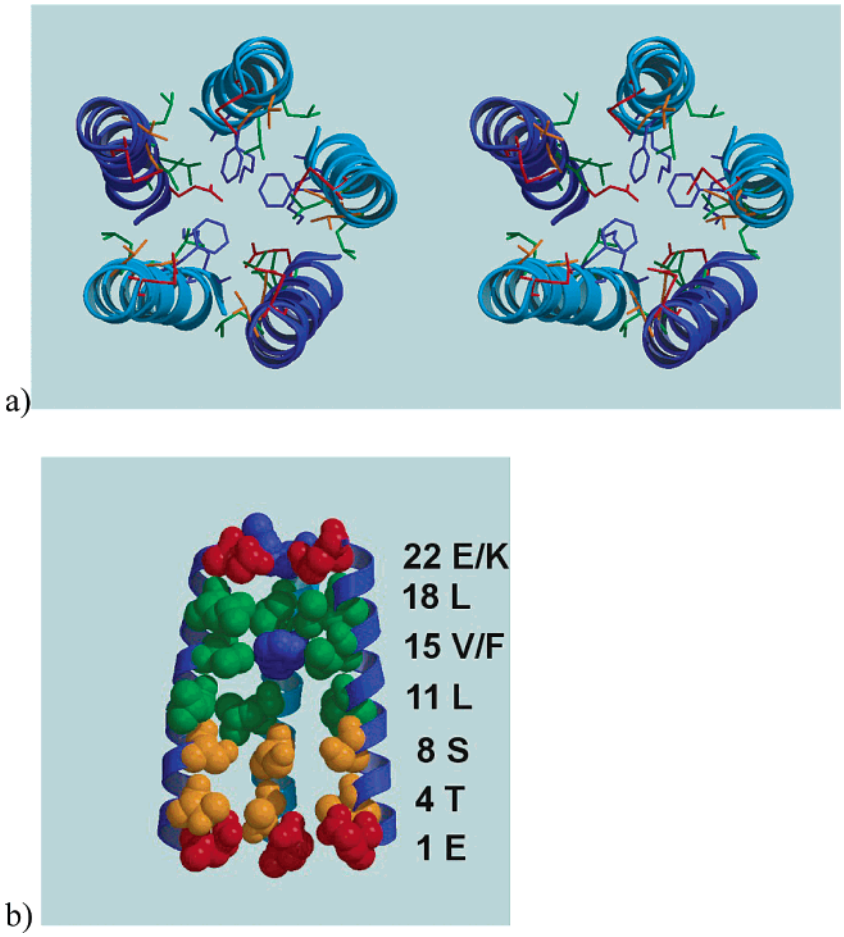

Figure 3. Graphical representation of the final model of the luminal domain of α3β4 nAChR. The α3 helices are colored in blue, and β4 helices are in cyan. The residues lining the lumen of the channel are shown explicitly. Charged residues are shown in red and blue. Hydrophobic residues are shown in green. Hydrophilic residues are shown in orange, and the phenylalanine from β4 is shown in blue: (a) top view in stereo mode (intracellular side) with exposed residues rendered in wireframe mode; (b) side view of the channel with the α3, β4, and α3 helices shown from left to right. Two of the β4 helices have been removed for clarity. Exposed residues are rendered in CPK mode. Labels show the numbering of rings according to Table 1.

field,[51] as implemented in AutoDock. The van der Waals and electrostatic interactions were computed using Lennard-Jones (12-6) and Coulomb type energy functions, respectively.[56] The angular dependent functional form (12-10) was used to model the H-bonded interactions. The modified genetic algorithm−local search (GALS)[54] method was used in this study, and the parameters are summarized in the Supporting Information. AutoDockTools,[57] a graphical user interface, was used to set up, run, and analyze the AutoDock runs.

3. Results and Discussion

3.1. Affinity Chromatography Results. In this study, 20 known NCIs with diverse molecular structures (Figure 2) were chromatographed on the α3β4 nAChR column. All but two of these compounds produced very broad, highly asymmetric peak profiles consistent with specific binding interactions with the immobilized nAChR. Representative peak profiles for two known NCIs (ketamine and MK-801) are presented in Figure 4 (profiles A and B, respectively).

Application of the nonlinear chromatographic technique to chromatographic traces produces four different parameters describing the retention process:[28] thermodynamic capacity factor k', association rate constant

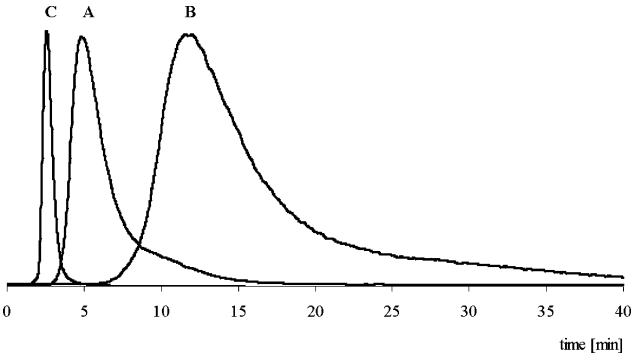

Figure 4. Comparison of peak profiles of ketamine (A) and MK-801 (B) with the profile of negative control phenylbutazone (C). Signals are rescaled to compare shapes.

(k_{on}) and dissociation constant rate constant (k_{off}) for the ligand−receptor complex, and the equilibrium constant for complex formation (K). These parameters were obtained for the 18 NCIs that eluted from the column (see Table 2).

Two of the NCIs (chlorpromazine and quinacrine) did not produce observable peaks under the chromatographic conditions used in this study. Both of these compounds have been identified as effective NCIs with IC_{50} values of 1.0−3.0 μM.[58,59] Chlorpromazine has been characterized as binding in the internal lumen of the

Table 2. Chromatographic Parameters of Tested Compounds Obtained Using Immobilized α3β4 nAChR Column

	k'	k_{on} ($\mu M^{-1} s^{-1}$)	k_{off} (s^{-1})	K (μM^{-1})
amantadine	9.0	30.8	6.73	4.6
bupropion	13.0	28.7	5.14	5.6
chlorpromazine				
clozapine	155.2	24.8	0.55	44.8
dilthiazem	43.5	26.8	1.60	16.8
ethidium	191.8	35.9	0.18	199.8
ketamine	8.2	38.4	8.50	4.5
laudanosine	22.9	25.0	2.18	11.5
mecamylamine	10.9	40.1	5.96	6.7
memantine	16.7	18.8	3.45	5.5
methadone	44.4	15.9	1.37	11.6
methamphetamine	8.4	29.1	6.81	4.3
MK-801	19.1	27.1	3.48	7.8
phenylcyclidine	24.1	23.2	2.69	8.6
quinacrine				
dextromethorphan	61.3	23.7	1.01	23.4
levomethorphan	35.8	18.6	1.55	12.0
dextrorphan	26.8	20.7	2.30	9.0
(+)-3-methoxymorphinan [3-MM]	56.5	18.8	1.00	18.9
(+)-3-hydroxymorphinan [3-OM]	26.4	14.3	1.97	7.3
Control Compounds				
acetaminophen	5.3	8.4	17.17	0.5
acetanilide	5.9	8.2	25.54	0.3
3,4-dimethoxybenzoic acid	4.5	9.8	18.21	0.5
2,4-dinitrobenzoic acid	7.7	9.1	12.12	0.7
phenylbutazone	6.3	8.7	22.22	0.4

nAChR.[5] It is not clear why this compound did not produce a chromatographic trace.

Unlike the majority of NCIs employed in this study, the primary binding site for quinacrine is located in the nonannular lipid domain on the border between the receptor and the membrane and not the luminal domain.[60] The results most likely reflect an extremely slow dissociation of quinacrine from this binding site.

The five negative controls used in this study produced very sharp, symmetric peaks with retention factors significantly lower than those of the NCIs, and a representative profile for phenylbutazone is presented in Figure 4 (profile C). The chromatographic traces of the controls reflect the fact that they do not significantly interact with the active site of the nAChR. Although the nonlinear chromatography approach assumes that strong ligand−receptor interactions occur at the single site, the method was used to analyze the chromatographic profiles of the control compound (Table 2). The chromatographic parameters derived for control compounds were compared with these derived for NCIs, and in each instance k', k_{on}, and K values were lower while k_{off} values were higher for controls. A comparison of the data illustrates that NCIs significantly interact with the chromatographic phase and provide minimum parameters for this interaction.

The chromatographic experiments were conducted using reversed-phase ion chromatographic conditions, which are defined as a polar (aqueous) mobile phase and a charged stationary phase. Under these conditions, it could be expected that the lipophilicity of the solutes would also play a role in the retention process. However, previous studies with the α3β4 affinity column demonstrated that lipophilicity does not significantly contribute to the observed chromatographic retention.[28] The data from this study were consistent with these results because the observed k' values for the experimental and control compounds were not correlated with calculated c log P values. For example, the c log P value for phenylbutazone (a neutral compound) was 3.95, and the observed k' was 6.3 while the c log P values for the NCIs mecamylamine and phenylcyclidine were 2.51 and 4.54 and the k' values were 10.9 and 24.1, respectively. It is of interest to note that the calculated c log P values for quinacrine and chlorpromazine were 4.9 and 3.8, respectively, and that this parameter did not appear to play a role in the inability to detect chromatographic profiles of these compounds.

Chromatographic retention on an affinity-based column is the summation of specific and nonspecific interactions, which occur during the chromatographic process. The results from this study indicate that the chromatographic retention of the negative controls was a result of nonspecific interactions with the protein surface and the chromatographic backbone and that these interactions do not have a significant impact on the retentions of the NCIs on the α3β4 affinity column.

This assumption is supported by the enantioselective separation of levomethorphan and dextromethorphan on the α3β4 nAChR affinity column.[29] Previous studies on chromatographic chiral recognition mechanisms have established that observed enantioselective separations are the result of specific but unequal interactions with a chiral selector, in this case the immobilized nAChR, and not the chromatographic backbone (cf. refs 61 and 62).

The primary role of luminal NCI−nAChR interactions in the nonlinear chromatographic process was also supported by the results obtained using a series of compounds related to dextromethorphan, (+)-3-hydroxy-*N*-methylmorphinan (dextrorphan), (+)-3-hydroxymorphinan (3-OM), and (+)-3-methoxymorphinan (3-MM). In this study, the k' values for the O-demethylated derivatives dextrorphan and 3-OM were over 50% less than the k' values for the O-methylated derivatives dextromethorphan and 3-MM (Table 2). Under the chromatographic conditions, the phenoxy moieties of the dextrorphan and 3-OM molecules will be partially ionized. Since the internal surface of the ion channel is highly polar and negatively charged, the resulting negative charge should destabilize the dextrorphan−nAChR and 3-OM−nAChR complexes relative to the complexes formed by dextromethorphan and 3-MM.

The calculated association (k_{on}) and dissociation (k_{off}) rate constants support this analysis (Table 2). There was no significant difference in the k_{on} values calculated for dextromethorphan, dextrorphan, and 3-MM, while for 3-OM this parameter was reduced by 40% relative to dextromethorphan. However, significant differences were observed between the calculated k_{off} values for dextromethorphan and 3-MM and those calculated for dextrorphan and 3-OM. The O-demethylated compounds dissociated twice as quickly.

Previous competitive displacement studies with the NCIs mecamylamine, bupropion, ketamine, and dextromethorphan have also demonstrated that these compounds compete at the same high-affinity site on the α3β4 nAChR, the channel lumen within the central pore.[28] Thus, in the first approximation, the nonlinear chromatographic parameters calculated for the known NCIs are a specific reflection of NCI−nAChR binding at the channel lumen.

Table 3. QSAR Equations Describing Chromatographic Parameters[a]

$\log k' = 5.255(\pm0.942) + 0.491(\pm0.092)E_{HOMO} + 0.0118(\pm0.0049)S_{YZ}$ $r = 0.894$, $s = 0.168$, $F = 27.929$, $n = 17$	eq 1
$\log k_{on} = 7.693(\pm0.111) - 0.00787(\pm0.00257)S_{YZ} + 0.0700(\pm0.0237)\text{HA} - 0.00276(\pm0.00118)\text{TPSA}$ $r = 0.762$, $s = 0.0883$, $F = 5.997$, $n = 17$[b]	eq 2
$\log k_{off} = -3.096(\pm0.926) - 0.454(\pm0.090)E_{HOMO} - 0.0128(\pm0.00471)S_{YZ}$ $r = 0.891$, $s = 0.165$, $F = 26.961$, $n = 17$	eq 3
$\log K = 11.412(\pm0.604) + 0.492(\pm0.0669)E_{HOMO}$ $r = 0.885$, $s = 0.135$, $F = 54.130$, $n = 17$	eq 4

[a] E_{HOMO} is the highest occupied molecular orbital energy calculated with MOPAC as implemented in Cerius2.[42] S_{YZ} is the area of the molecular shadow projected in the *YZ* plane. HA is the number of hydrogen bond acceptors. TPSA is the total polar surface area. [b] Outlier is mecamylamine as identified by the standardized residual value being >2.

3.2. QSAR Models of Chromatographic Data. During the development of the QSAR models, over 80 structural descriptors were calculated and each individual descriptor was correlated against the nonlinear chromatographic parameters. This process identified ethidium as an outlier in a significant number of comparisons. Ethidium is a high-affinity noncompetitive inhibitor, but this is the only compound in the series that is postulated to bind at a site in the outer vestibule of the ion channel about 46 Å above the transmembrane portion of the receptor.[5,15] The other NCIs used in this study bind to site(s) inside the central lumen of the nAChR. Ethidium was also the only permanently ionized compound in the cassette. Thus, it was not surprising that ethidium appeared as an outlier in the QSAR analyses and this compound was not included in the determination of the final QSAR equations.

The results of the QSAR analyses are presented in Table 3. Each of the derived equations contain a descriptor related to the electronic properties of the NCIs, E_{HOMO}, or total polar surface area (TPSA). This is consistent with the fact that NCIs bind at the internal surface of the nAChR ion channel, which is highly polar and negatively charged. Three of the four equations also contain a shape descriptor (S_{YZ}), which is consistent with the fact that the NCIs bind within a defined space on the receptor. Thus, the QSAR analysis describes a chromatographic and, as discussed above, an NCI−receptor process where the primary driving force is electrostatic interactions between positively charged ligands and a negatively charged nAChR, which take place in the structurally defined central pore of the receptor.

Three of the four derived equations, eqs 1, 2, and 4, are statistically significant with *r* values of 0.89 and *F* values greater than 21. Cross-validated r^2 values determined by the leave-one-out method for these equations were 0.630, 0.697, and 0.739, respectively. It is assumed that these equations could be used to predict relative k', k_{off}, and K_a values for a wide variety of potential NCIs of the α3β4 nAChR. Although it is statistically valid, eq 2 has limited predictive power because of its low *r* and *F* values. The weakness of this correlation stems in part from the high level of inherent experimental error associated with the determination of k_{on}. While the other nonlinear chromatography parameters were determined directly from the fitting procedure to chromatographic traces, the k_{on} values used in this study were indirectly calculated from k_{off} and *K*, which aggregated the experimental errors.[28]

The QSAR models developed in this study do not contain a chiral descriptor and obviously cannot predict the enantioselective interaction of dextromethorphan and levomethorphan with the nAChR. Therefore, it was necessary to develop a method to explore the three-dimensional description of the ligand−receptor interaction, which is discussed below.

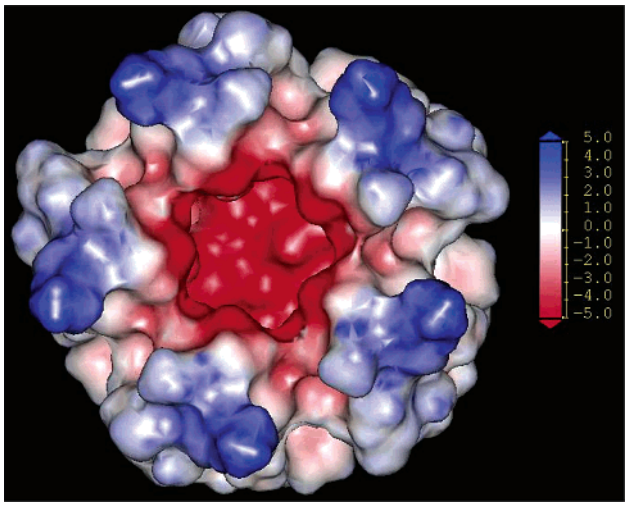

Figure 5. Map of the electrostatic potential of the solvent-accessible surface of the α3β4 nAChR channel. Negative potentials are shown in red, and the positive potentials are shown in blue.

3.3. Results of Docking Simulations of NCIs into the Model of α3β4 nAChR. The molecular model of the α3β4 nAChR luminal domain suggests that there are a significant number of possible sites where NCIs might bind. A series of 39 molecular structures derived from the 17 NCIs and 5 negative controls used in the affinity chromatography experiments were docked into the model of the α3β4 nAChR using AutoDock. For the 17 NCI ligands, both the neutral and protonated forms of the molecules were used in the docking simulations. The five control molecules were docked in the neutral form only, since they were chosen to be nonprotonated under the experimental conditions. Distinctively different docking interactions were found for the protonated and neutral states of NCI molecules.

Electrostatic interactions are a key factor in the interaction of NCIs with the nAChR channel,[15] which is illustrated by the electrostatic potential mapped on the solvent-accessible surface of the α3β4 nAChR model (Figure 5). One should note that the internal surface of the lumen domain is highly electron-rich, a feature that appears to be responsible for the cation selectivity as well as for strong interactions with positively charged NCIs. Electrostatic interactions are also reflected in the QSAR models presented above, where electronic proper-

Table 4. Quantitative Description (Docked Energy ΔE, Estimated Free Energy of Binding ΔG, and Estimated Inhibition Constant K_i) of Lowest Energy Docked Conformation for Each Ligand Docked in Neutral (n) and Protonated (+) State

ligand name	docked energy (kcal/mol)		estimated ΔG (kcal/mol)		estimated inhibition constant K_i (mol)	
	$\Delta E_{(n)}$	$\Delta E_{(+)}$	$\Delta G_{(n)}$	$\Delta G_{(+)}$	$K_{i(n)}$	$K_{i(+)}$
amantadine	−6.24	−10.59	−5.91	−10.95	4.67×10^{-5}	1.72×10^{-8}
bupropion	−7.08	−11.51	−6.47	−12.02	1.82×10^{-5}	3.68×10^{-9}
clozapine	−10.07	−12.39	−9.22	−12.82	1.74×10^{-7}	8.22×10^{-10}
dilthiazem	−10.67	−12.71	−8.22	−14.91	9.45×10^{-7}	4.79×10^{-10}
ketamine	−3.95	−11.12	−6.08	−9.26	3.50×10^{-5}	7.09×10^{-9}
laudanosine	−9.16	−11.96	−7.69	−13.63	2.31×10^{-6}	1.70×10^{-9}
mecamylamine	−6.10	−11.50	−6.41	−11.35	2.00×10^{-5}	3.69×10^{-9}
memantine	−6.93	−11.01	−6.61	−11.35	1.43×10^{-5}	8.55×10^{-9}
methadone	−6.26	−11.65	−7.05	−10.90	6.76×10^{-6}	2.90×10^{-9}
methamphetamine	−6.39	−10.42	−5.52	−11.39	8.93×10^{-5}	2.16×10^{-8}
MK-801	−7.41	−11.41	−7.41	−11.41	3.73×10^{-6}	4.36×10^{-9}
phenylcyclidine	−6.14	−11.19	−7.58	−10.33	2.79×10^{-6}	6.22×10^{-9}
dextromethorphan	−8.84	−11.87	−8.73	−11.98	3.98×10^{-7}	1.99×10^{-9}
levomethorphan	−8.52	−12.27	−8.40	−12.40	6.91×10^{-7}	1.02×10^{-9}
dextrorphan	−8.38	−12.04	−8.06	−12.36	1.24×10^{-6}	1.49×10^{-9}
3-MM	−8.37	−11.93	−8.25	−12.07	8.92×10^{-7}	1.81×10^{-9}
3-OM	−8.00	−12.09	−7.71	−12.41	2.24×10^{-6}	1.37×10^{-9}
Control Compounds						
acetanilide	−5.76		−5.17		1.63×10^{-4}	
acetaminophen	−6.00		−5.06		1.96×10^{-4}	
2,4-dinitrobenzoic acid	−6.48		−4.94		2.39×10^{-4}	
3,4-dimethoxybenzoic acid	−5.90		−5.35		1.21×10^{-4}	
phenylbutazone	−6.82		−6.44		1.91×10^{-5}	

ties of the ligand associated with its charge state were strongly correlated with the observed affinity. Therefore, the protonated states of the 17 ligand molecules were initially used in the docking simulations. The simulations of each ligand produced several clusters of orientations located in the polar region of the lumen in proximity to the charged glutamic acid residues of the intermediate ring. There were no significant differences in the docked energies of the various clusters. These results suggest that nonspecific electrostatic interactions with negatively charged groups were the dominant interactions rather than specific interactions at a defined site. The electrostatic interactions were observed throughout all of the docking simulations of the protonated NCIs, and the ligand orientations were concentrated in the region of the E ring with no specific orientation being observed for the lowest energy orientations.

The lowest energy orientation for each ligand can be characterized by several quantitative parameters. The results from the AutoDock simulations are reported in terms of docked energy values (ΔE) as well as the estimation of free energy of binding (ΔG) and estimated inhibition constants (K_i).[54] These parameters, determined for the lowest energy orientation of each of the 17 protonated NCIs, are presented in Table 4.

The simulations of neutral NCIs revealed that they bind in quite different positions within the channel compared to their protonated forms. The neutral NCIs bind deeper in the channel predominantly in the nonpolar region near the V/F ring (position 15). The unique pocket formed by the cleft between the phenyl ring introduced by phenylalanine in the β4 subunit and the isopropyl moiety from the valine in the α3 subunit is a primary binding pocket for the hydrophobic moieties of all of the NCIs studied here. When the nonpolar part of the inhibitor sits in this hydrophobic pocket, the polar part of the ligand can interact with nearby polar residues exposed to the lumen (e.g., the S ring) to form hydrogen bonds. We speculate that this interaction may be unique to this specific subtype, since sequences lacking the bulky F residue in position 15 would not possess this prominent binding site (see Table 1). Figure 6 presents the stereoview of the cleft formed in the lipophilic portion of the channel between V(α3) and F(β4). Two quasi-symmetrical clefts can be found in the model; thus, there are two sites at which the energy of ligand interaction should be approximately equal.

The quantitative descriptions of the lowest energy conformation for each ligand tested in the neutral state ($\Delta E_{(n)}$, $\Delta G_{(n)}$, and $K_{i(n)}$) are presented in Table 4.

The five negative controls included in the chromatographic study were also docked into the lumen model. As previously discussed, only the neutral states of the molecules were docked. The negative control molecules formed scattered clusters in their final docking orientations along the channel where interactions with V/F and L rings or G ring were predominant with no single orientation of binding dominating. Table 4 shows that these compounds have calculated inhibition constants higher than the known NCIs, consistent with the observed scatter in binding orientation. Thus, the simulation model can be used to sort out compounds, which do not significantly interact with the lumen and should not have inhibitory properties.

3.4. Correlation of the Docking Results with the Chromatographic Parameters. The docking data were related to experimental parameters determined for the NCIs in the nonlinear affinity chromatography experiments. Table 5 presents correlation equations between the logarithm of the estimated inhibition constant (K_i) obtained in the docking of either neutral or protonated ligands and three chromatographic parameters (log k', log k_{off}, and log K). These parameters were found to be strongly correlated with the results of docking simulations, whereas the fourth parameter obtained in chromatographic analysis (association rate constant (k_{on})) has shown no correlation.

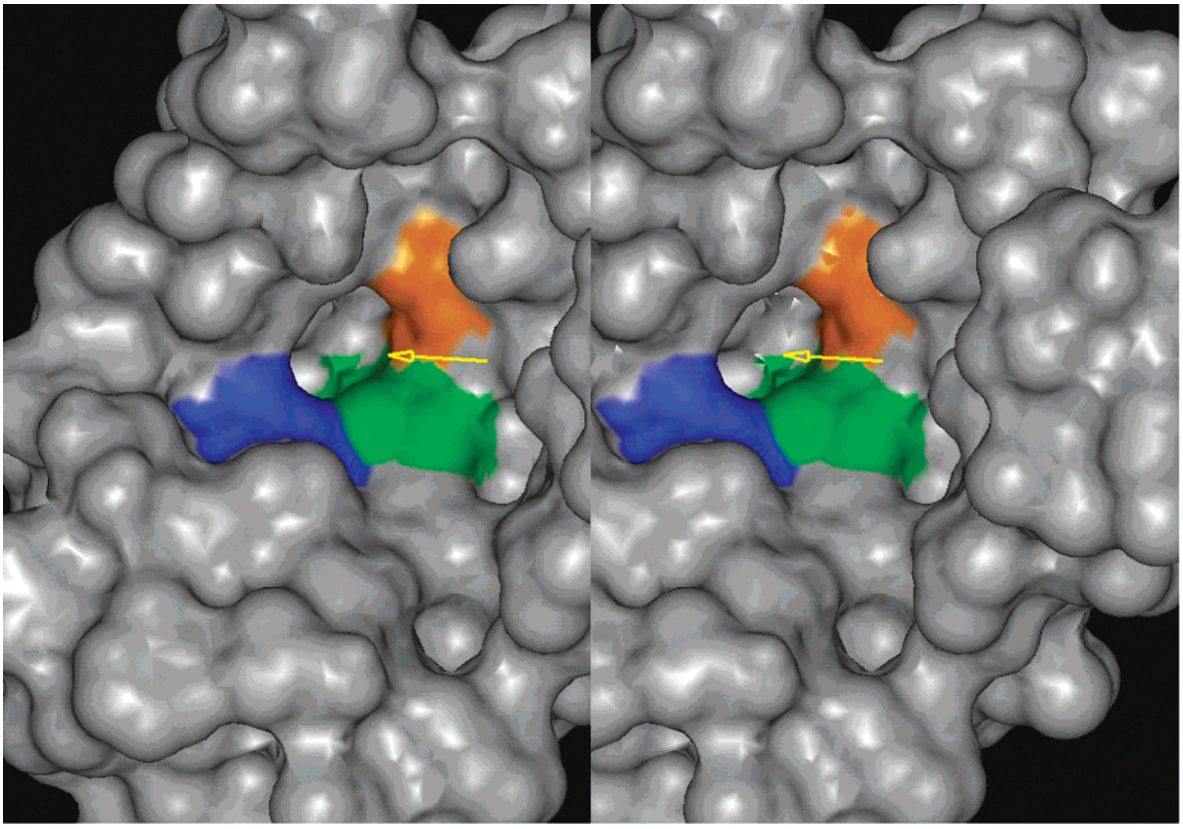

Figure 6. Stereoview of the hydrophobic part of the α3β4 nAChR channel with depiction (indicated with yellow arrow) of the cleft formed between phenylalanine (blue) and valine (green) and serine (orange), identified as a binding pocket for the neutral form of NCIs. The receptor is viewed from the top and rendered with the solvent-accessible area. For clarity the hydrophilic portion of two helices has been removed.

Table 5. Equations Describing Correlations between Estimated Inhibition Constant Simulated by Docking of NCI Ligand in Either Protonated {$\log(1/K_{i(+)})$} or Neutral {$\log(1/K_{i(n)})$} State with the Experimental Chromatographic Parameters: log k', log k_{off}, and log K[a]

	equation	r	cv r^2	s	F
k'	$\log k' = 0.59(\pm0.13)\log(1/K_{i(+)}) - 3.6(\pm1.1)$[b]	0.767	0.474	0.232	21.47
	$\log k' = 0.41(\pm0.05)\log(1/K_{i(n)}) - 0.84(\pm0.05)$[c]	0.918	0.796	0.145	79.95
k_{off}	$\log k_{off} = -0.57(\pm0.12)\log(1/K_{i(+)}) + 5.3(\pm1.0)$	0.767	0.482	0.225	21.47
	$\log k_{off} = -0.40(\pm0.04)\log(1/K_{i(n)}) + 2.6(\pm0.2)$[c]	0.918	0.810	0.138	80.84
K	$\log K = 0.47(\pm0.10)\log(1/K_{i(+)}) + 2.98(\pm0.88)$[b]	0.761	0.459	0.188	20.60
	$\log K = 0.32(\pm0.04)\log(1/K_{i(n)}) + 5.2(\pm0.2)$	0.903	0.754	0.125	66.12

[a] cv r^2 is the cross-validated r^2 determined by the leave-one-out method. [b] Outlier is clozapine as identified by the standardized residual value being >2. [c] Outlier is methadone as identified by the standardized residual value being >2.

Since the standard models assume that the NCIs are protonated during the blocking of the channel,[15] it should be expected that docking of the ionized form of the ligands should produce results better correlated with experimental affinities. As shown in Table 5, this expectation was wrong. The strength of the correlations can be judged by comparison of r, s, or F values associated with each equation. Simulations of neutral ligands gave stronger correlation with chromatographic data ($r > 0.9$; $F > 60$) than those developed using the protonated ligands ($r \approx 0.76$; $F \approx 20$). Moreover, docking experiments with the protonated NCIs show some serious inconsistencies. For example, the results of the docking experiments did not reflect the enantioselective differences between dextromethorphan and levomethorphan. In addition, the chromatographic capacity factors (k values) of the dextromethorphan congeners were experimentally determined as dextromethorphan > 3-MM > levomethorphan > dextrorphan = 3-OM (Table 2). Docking simulations of the protonated NCIs predicted a completely different order: levomethorphan > 3-OM ≥ dextrorphan> 3-MM > dextromethorphan (Table 4).

In contrast to protonated ligands, docking results of neutral molecules were significantly better correlated with the experimental data. This suggests that the interactions with the neutral state of the NCI were responsible for the differences seen in the affinity chromatography experiments. This hypothesis is supported by the fact that the enantiospecificity between dextromethorphan and levomethorphan was successfully explained when they were docked in their neutral states (see section 3.5). In addition, the $\Delta G_{(n)}$ values derived in the neutral docking studies for dextromethorphan and its analogues were consistent with the results from the affinity chromatography study, i.e., dextromethorphan > levomethorphan > 3-MM > dextrorphan > 3-OM.

3.5. Enantioselective Interactions of Levomethorphan and Dextromethorphan. In this study, the

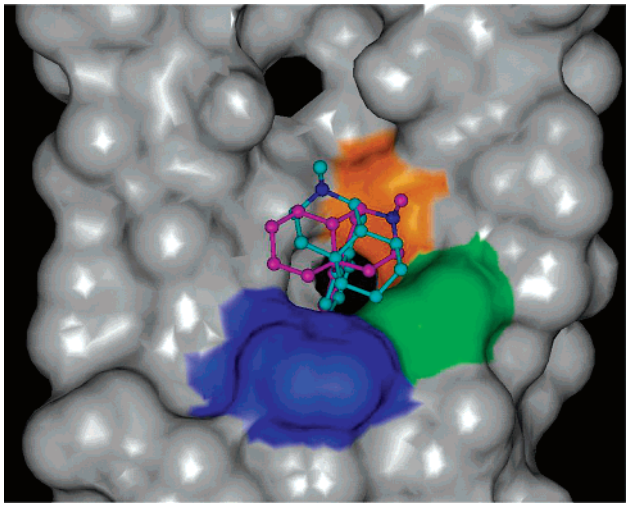

Figure 7. Overlay of the most stable docked orientations of dextromethorphan (cyan) and levomethorphan (magenta) complexes. Nitrogen atoms of both enantiomers are colored in blue. The binding pocket formed between β4 and α3 helices is shown in detail to highlight the interactions leading to an enantioselectivity. Residues forming the cleft are color-coded as in Figure 6.

docking simulations of the neutral dextromethorphan and levomethorphan ligands provide a possible explanation for the molecular basis of the observed enantioselectivity. Since dextromethorphan and levomethorphan have the same overall physicochemical properties, the observed enantioselectivity must be due to specific asymmetric binding interactions with a defined site(s) of the receptor. In the model of the central lumen developed in this study, the lowest energy docked conformations of the neutral complexes are located at the V/F cleft (Figure 7). The mirror image relationship between the two enantiomers and their lack of conformational mobility produces two unique orientations, which result in distinctly different interactions with nearby amino acid moieties comprising the lumen. In the case of dextromethorphan, the bridgehead nitrogen atom is oriented toward the hydroxy moiety on the serine residue (position 12) located on the α3 helix, which increases the probability of H-bond interaction. With levomethorphan, the bridgehead nitrogen atom is pointing away from the two helices forming the α3 and β4 subunits because of the steric considerations, which reduces the probability and strength of any H-bond interaction. The calculated difference in methorphan−nAChR complexes, $\Delta\Delta G_{(n)}$ derived by $\Delta G_{DM} - \Delta G_{LM}$, was −0.33 kcal/mol in favor of dextromethorphan. This energy value is in agreement with the experimental value obtained from thermodynamic chromatography studies[29] where the experimental $\Delta\Delta G°$ was reported to be −0.29 kcal/mol.

On the basis of the results from the docking experiments, the V/F cleft appears to play a key role in the enantioselective binding of dextromethorphan and levomethorphan to the α3β4 nAChR. This particular hydrophobic pocket is a unique feature of the α3β4 nAChR and should differ from the binding area produced by the V/V moieties present in the non-β4-containing nAChR subtypes. This hypothesis is consistent with the preliminary results from a chromatographic study utilizing an immobilized α3β2 nAChR column, which showed a significantly lower enantioselectivity for dextromethorphan and levomethorphan compared to the immobilized α3β4 nAChR column. The enantioselective separation (α) observed on the immobilized α3β2 nAChR was 1.03, which reflects a free energy difference ($\Delta\Delta G°$) of −0.02 kcal/mol between the two complexes (data to be published), compared to an α = 1.62 and a $\Delta\Delta G°$ of −0.29 kcal/mol obtained on the immobilized α3β4 nAChR column.[29] These data, taken together with the relative binding affinities for the dextromethorphan congeners, lend strong support for the location of NCI binding in the lumen of the nAChR channel as well as the relative energies predicted by the docking simulations.

4. Conclusion

The results from the nonlinear chromatographic studies on the immobilized nAChR column describe the physical relationships between a compound and the immobilized receptor (drug binding). The nonlinear chromatographic parameters determined in these studies were obtained in a dynamic system but under simplified conditions when compared to a cell-based functional assay (i.e., no neurotransmitter stimulation, no transmembrane potential, etc.). However, our previous studies showed that the binding process plays a significant role in the functional properties of the NCIs. It was established that chromatographically determined k_{off} can be related to the length of nAChR inhibition determined in a cell-based functional assay.[28,29] The present study has extended this observation through the determination of a QSAR (eq 3), which can be used to assess relative k_{off} values, although the inability to predict the enantioselective functional difference between dextromethorphan and levomethorphan demonstrated a general weakness in the approach. However, it appears that the nonlinear chromatographic/QSAR approach developed in this study can be used to qualitatively screen the noncompetitive inhibitory potential of a compound and be of use in the drug discovery and development processes. This possibility will be discussed elsewhere.

The work presented here also explored the detailed molecular interactions between the α3β4 nAChR and luminal NCIs, which act as channel blockers. A new molecular model of the lumen specific to α3β4 nAChR has been elaborated, and the model shares commonly known structural properties with previously reported molecular models of the transmembrane domain of nAChR. However, some features specific to the α3β4 subtype of the receptor have been found. In particular, the model has identified a hydrophobic binding site, the V/F cleft, and the docking studies have demonstrated the key role this site plays in the stabilization of NCI−α3β4 nAChR complexes.

Docking simulations using the molecular model of the lumen specific to α3β4 nAChR were performed using both neutral and protonated NCIs, and distinctly different modes of binding were found. Protonated NCIs interacted primarily with a ring of negatively charged residues (intermediate ring, position 1), while the neutral ligands were bound to the lumen at the V/F cleft. Both sets of results were correlated with data

obtained from chromatographic experiments. However, while the results from the docking of the protonated NCIs showed some correlation with experiment, the simulations on the neutral NCIs yielded much better correlations and were more consistent with the observed enantioselectivity and congeners affinities. Moreover, docking of neutral forms of NCIs seems to have a higher predictive power to model affinity chromatography data than the QSAR models. For example, the chromatographic log k' parameter was modeled by the QSAR equation with a cross-validated r^2 value of 0.630, whereas the model of neutral docking produced a correlation with a cross-validated r^2 value of 0.796.

A significant observation is that docking of neutral ligands provided a molecular explanation for the experimentally observed enantiodiscrimination between dextromethorphan and levomethorphan with α3β4 nAChR. The docking simulations suggest that the interaction with the cleft created by the V/F ring is essential for enantioselective discrimination. This observation is supported by chromatographic experiments involving the immobilized α3β2 subtype of nAChR (β2 position 15 is V instead of F), where markedly lower selectivity of this pair of methorphan enantiomers was seen.

The interpretation of the docking results and their relationship to the experiment data derived from the affinity chromatographic studies suggest an alternative mechanism of inhibition by noncompetitive luminal channel blockers. As a first approximation, it can be envisioned that the mechanism of NCI inhibition is associated with the strong electrostatic interaction between the negatively charged surface of the lumen (Figure 5) and the positively charged drug molecules.[15] Most NCIs are protonated under the conditions of the chromatographic experiments, but neither the docking simulations of the protonated states of the inhibitors nor the QSAR models properly predicted the experimentally observed enantioselectivity of dextromethorphan and levomethorphan with the α3β4 nAChR channel. In contrast, the results of the docking of the neutral ligands correlated better with the experimental data and accurately reflected the observed relative affinities, including the enantioselective binding of dextromethorphan and levomethorphan. Taking this into account, one may hypothesize that the interaction of a NCI with the α3β4 nAChR proceeds in three steps:

(1) The negatively charged regions of the receptor's lumen attract the protonated inhibitor.

(2) The proton from the NCI is transferred to one of the negatively charged residues as the NCI enters the channel.

(3) The neutral NCI travels down the channel and binds at the apolar inner region of the lumen, the V/F cleft.

The screening of drug candidates for NCI activity against nAChRs is not a standard procedure in the drug development process. The results of the chromatographic and molecular modeling studies indicate that the combined model may be useful in the creation of other luminal models of nAChR subtypes in the in silico prediction of side effects due to noncompetitive binding at these receptors and as a tool in new drug discovery.

Experimental Section

Materials. HPLC grade methanol, ammonium acetate, and 0.1 M ammonium hydroxide were purchased from Fisher Scientific (Pittsburgh, PA).

Figure 2 presents ligands tested on α3β4 nAChR column. The compounds were purchased from Sigma-Aldrich Co. (St. Louis, MO) with the exception of dextromethorphan metabolites (dextrorphan, 3-MM, and 3-OM), which were kindly donated by Hoffmann LaRoche (Nutley, NJ), and levomethorphan, which was purchased from Cerilliant Co. (Round Rock, TX).

Chromatographic System. Preparation of the α3β4 nAChR column was described earlier.[28,29] In brief, the KXα3β4R2 cell line with expressed α3β4 nAChR was used to create the column. The transfected cells were suspended in 50 mM Tris-HCl, pH 7.4, (buffer A), homogenized for 30 s with a Brinkmann Polytron, and centrifuged at 35000*g* for 10 min at 4 °C. The pellet was resuspended in 6 mL of 2% cholate in buffer A, and the mixture was stirred for 2 h. The mixture was centrifuged at 35000*g* for 30 min, and the supernatant containing nAChR−cholate solution was collected.

The receptors were immobilized on an immobilized artificial membrane (IAM) stationary phase (IAM-PC [12 μm, 300 Å], Regis Chemical Co., Morton Grove, IL). To do this, dried IAM particles were suspended in 4 mL of the detergent solution containing the nAChR proteins and the mixture was stirred for 1 h at room temperature. The suspension was then dialyzed against 2 × 1 L of buffer A for 24 h at 4 °C. The nAChR−IAM support was then washed with buffer A and centrifuged, and the solid was collected and packed into a 0.5 cm (i.d.) × 0.8 cm HR5/2 glass column purchased from Amersham Pharmacia Biotech (Uppsala, Sweden).

The LC−MS system composed of a LC10AD pump (Shimadzu, Columbia, MD), ESA 540 autoinjector (Spark-Holland), and a Micromass Q TOF mass spectrometer (Micromass, Beverly, MA). The data were recorded and processed using MassLynx, version 3.5 (Micromass). The mobile phase was composed of buffer (10 mM ammonium acetate, pH 7.4) modified with methanol in a ratio of 85:15 (v/v) buffer/methanol. The flow rate of the mobile phase was 0.2 mL/min.

Samples of 10 μM aqueous solutions of each compound were prepared. After equilibration of the column (approximately 2 h), an amount of 20 μL of each solution was subsequently injected into the column and the chromatograms were detected with the positive ionization mass spectometry method (ESI+). The molecular weight + 1 (M + H) of each parent compounds were monitored.

The obtained chromatograms were smoothed and extracted to the Excel worksheet as a set of two columns: retention time and signal intensity. These input data were further processed with PeakFit software.[41] After standard linear baseline subtraction, each peak profile was subjected to a fitting procedure to the nonlinear chromatography impulse input solution function. The set of parameters (a0, a1, a2, and a3) describing each peak profile was used for the calculation of descriptors of the kinetics of NCI interaction with the nicotinic receptor immobilized on the column (k', k_{on}, k_{off}, and K).

Acknowledgment. The authors thank Kenneth L. Kellar and Yingxian Xiao (Georgetown University) for their guidance and insight regarding noncompetitive inhibitors of the nAChR.

Supporting Information Available: Molecular descriptors used in QSAR models, details of docking calculations, and atomic coordinates of molecular model of target receptor. This material is available free of charge via the Internet at http://pubs.acs.org.

References

(1) Changeux, J.-P.; Bertrand, D.; Corringer, P. J.; Dehaene, S.; Edelstein, S.; Lena, C.; Le Novere, N.; Marubio, L.; Picciotto, M.; Zoli, M. Brain nicotinic receptors: structure and regulation, role in learning and reinforcement. *Brain Res. Rev.* **1998**, *26*, 198−216.

(2) Karlin, A. Emerging structure of the nicotinic acetylcholine receptors. *Nat. Res. Neurosci.* **2002**, *3*, 102−114.
(3) Holladay, M. W.; Dart, M. J.; Lynch, J. K. Neuronal nicotinic acetylcholine receptors as targets for drug discovery. *J. Med. Chem.* **1997**, *40*, 4170−4194.
(4) Albuquerque, E. X.; Alkondon, M.; Pereira, E. F. R.; Castro, N. G.; Schrattenholz, A.; Barbosa, C. T. F.; Bonfante-Cabarcas, R.; Aracava, Y.; Eisenberg, H. M.; Maelicke, A. Properties of neuronal nicotinic acetylcholine receptors: pharmacological characterization and modulation of synaptic function. *J. Pharmacol. Exp. Ther.* **1997**, *280*, 1117−1136.
(5) Arias, H. R. Binding sites for exogenous and endogenous noncompetitive inhibitors of the nicotinic acetylcholine receptor. *Biochim. Biophys. Act.* **1998**, *1376*, 173−220.
(6) Hucho, F.; Tsetlin, V. I.; Machold, J. The emerging three-dimensional structure of a receptor. The nicotinic acetylcholine receptor. *Eur. J. Biochem.* **1996**, *239*, 539−555.
(7) Changeux, J.-P.; Galzi, J. L.; Devillers-Thiery, A.; Bertrand, D. The functional architecture of the acetylcholine nicotinic receptor explored by affinity labelling and site-directed mutagenesis. *Q. Rev. Biophys.* **1992**, *25*, 395−432.
(8) Millar, N. S. Assembly and subunit diversity of nicotinic acetylcholine receptors. *Biochem. Soc. Trans.* **2003**, *31*, 869−874
(9) Le Novere, N.; Corringer, P. J.; Changeux, J.-P. The diversity of subunit composition in nAChRs: evolutionary origins, physiologic and pharmacologic consequences. *J. Neurobiol.* **2002**, *53*, 447−456.
(10) Lloyd, K. G.; Williams, M. Neuronal nicotinic acetylcholine receptors as novel drug targets. *J. Pharmacol. Exp. Ther.* **2000**, *292*, 461−467.
(11) Gohlke, H.; Schwarz, S.; Gundisch, D.; Tilotta, M. C.; Weber, A.; Wegge, T.; Seitz, G. 3D QSAR Analyses-Guided Rational Design of Novel Ligands for the $(\alpha 4)_2(\beta 2)_3$ Nicotinic Acetylcholine Receptor. *J. Med. Chem.* **2003**, *46*, 2031−2048.
(12) Ferretti, G.; Dukat, M.; Giannella, M.; Piergentili, A.; Pigini, M.; Quaglia, W.; Damaj, M. I.; Martin, B. R.; Glennon, R. A. Homoazanicotine: a structure−affinity study for nicotinic acetylcholine (nACh) receptor binding. *J. Med. Chem.* **2002**, *45*, 4724−4731.
(13) Nielsen, S. F.; Nielsen, E. O.; Olsen, G. M.; Liljefors, T.; Peters, D. Novel potent ligands for the central nicotinic acetylcholine receptor: synthesis, receptor binding, and 3D-QSAR analysis. *J. Med. Chem.* **2000**, *43*, 2217−2226.
(14) Arias, H. R. Topology of ligand binding sites on the nicotinic acetylcholine receptor. *Brain Res. Rev.* **1997**, *25*, 133−191.
(15) Krauss, M.; Korr, D.; Herrmann, A.; Hucho, F. Binding properties of agonists and antagonists to distinct allosteric states of the nicotinic acetylcholine receptor are incompatible with a concerted model. *J. Biol. Chem.* **2000**, *275*, 30196−30201.
(16) Hernandez, S. C.; Bertolino, M.; Xiao, Y.; Pringle, K. E.; Caruso, F. S.; Kellar, K. J. Dextromethorphan and its metabolite dextrorphan block alpha3beta4 neuronal nicotinic receptors. *J. Pharmacol. Exp. Ther.* **2000**, *293*, 962−967.
(17) Fryer, J. D.; Lukas, R. J. Noncompetitive functional inhibition at diverse, human nicotinic acetylcholine receptor subtypes by bupropion, phencyclidine, and ibogaine. *J. Pharmacol. Exp. Ther.* **1999**, *288*, 88−92.
(18) Arias, H. R.; McCardy, E. A.; Gallagher, M. J.; Blanton, M. P. Interaction of barbiturate analogs with the *Torpedo californica* nicotinic acetylcholine receptor ion channel. *Mol. Pharmacol.* **2001**, *60*, 497−506.
(19) Lopez-Valdes, H. E.; Garcia-Colunga, J. Antagonism of nicotinic acetylcholine receptors by inhibitors of monoamine uptake. *Mol. Psychiatry* **2001**, *6*, 511−519.
(20) Xiao, Y.; Smith, R. D.; Caruso, F. S.; Kellar, K. J. Blockade of rat alpha3beta4 nicotinic receptor function by methadone, its metabolites, and structural analogs. *J. Pharmacol. Exp. Ther.* **2001**, *299*, 366−371.
(21) Fryer, J. D.; Lukas, R. J. Antidepressants noncompetitively inhibit nicotinic acetylcholine receptor function. *J. Neurochem.* **1999**, *72*, 1117−1124.
(22) Buisson, B.; Bertrand, D. Open-channel blockers at the human alpha4beta2 neuronal nicotinic acetylcholine receptor. *Mol. Pharmacol.* **1998**, *53*, 555−563.
(23) Slemmer, J. E.; Martin, B. R.; Damaj, M. I. Bupropion is a nicotinic antagonist. *J. Pharmacol. Exp. Ther.* **2000**, *295*, 321−327.
(24) Friederich, P.; Dybek, A.; Urban, B. W. Stereospecific interaction of ketamine with nicotinic acetylcholine receptors in human sympathetic ganglion-like SH-SY5Y cells. *Anesthesiology* **2000**, *93*, 818−824.
(25) George, T. P.; O'Malley, S. S. Current pharmacological treatments for nicotine dependence. *Trends Pharmacol. Sci.* **2004**, *25*, 42−48.
(26) Glick, S. D.; Maisonneuve, I. M.; Kitchen, B. A.; Fleck, M. W. Antagonism of alpha 3 beta 4 nicotinic receptors as a strategy to reduce opioid and stimulant self-administration. *Eur. J. Pharmacol.* **2002**, *438*, 99−105.
(27) Moaddel, R.; Wainer, I. W. Immobilized nicotinic receptor stationary phases: going with the flow in high-throughput screening and pharmacological studies. *J. Pharm. Biomed. Anal.* **2003**, *30*, 1715−1724.
(28) Jozwiak, K.; Haginaka, J.; Moaddel, R.; Wainer, I. W. Displacement and nonlinear chromatographic techniques in the investigation of interaction of noncompetitive inhibitors with an immobilized $\alpha 3\beta 4$ nicotinic acetylcholine receptor liquid chromatographic stationary phase. *Anal. Chem.* **2002**, *74*, 4618−4624.
(29) Jozwiak, K.; Hernandez, S. C.; Kellar, K. J.; Wainer, I. W. The enantioselective interactions of dextromethorphan and levomethorphan with the $\alpha 3\beta 4$-nicotinic acetylcholine receptor: comparison of chromatographic and functional data. *J. Chromatogr., B* **2003**, *797*, 373−379.
(30) Steinlein, O. K. Nicotinic acetylcholine receptors and epilepsy. *Curr. Drug Targets: CNS Neurol. Disord.* **2002**, *1*, 443−448.
(31) Sankararamakrishnan, R.; Adcock, C.; Sansom, M. S. P. The pore domain of the nicotinic acetylcholine receptor: molecular modeling, pore dimensions, and electrostatics. *Biophys. J.* **1996**, *71*, 1659−1671.
(32) Smith, G. R.; Sansom, M. S. P. Molecular dynamics study of water and Na^+ ions in models of the pore region of the nicotinic acetylcholine receptor. *Biophys. J.* **1997**, *73*, 1364−1381.
(33) Ortells, M. O.; Barrantes, G. E.; Wood, C.; Lunt, G. G.; Barrantes, F. J. Molecular modelling of the nicotinic acetylcholine receptor transmembrane region in the open state. *Protein Eng.* **1997**, *10*, 511−517.
(34) Barrantes, F. J. Lipid matters: nicotinic acetylcholine receptor−lipid interactions (review). *Mol. Membr. Biol.* **2002**, *19*, 277−284.
(35) Miyazawa, A.; Fujiyoshi, Y.; Unwin, N. Structure and gating mechanism of the acetylcholine receptor pore. *Nature* **2003**, *423*, 949−55.
(36) Ortells, M. O.; Barrantes, G. E. Understanding channel blocking in the nicotinic acetylcholine receptor. *Recept. Channels* **2001**, *7*, 273−288.
(37) Curtis, L.; Chiodini, F.; Spang, J. E.; Bertrand, S.; Patt, J. T.; Westera, G.; Bertrand, D. A new look at the neuronal nicotinic acetylcholine receptor pharmacophore. *Eur. J. Pharmacol.* **2000**, *393*, 155−163.
(38) Fornstedt, T.; Guiochon, G. Nonlinear effects in LC and chiral LC. *Anal. Chem.* **2001**, *73*, 608A−617A.
(39) Felinger, A.; Guiochon, G. Computer simulations in non-linear chromatography. *Trends Anal. Chem.* **1995**, *14*, 6−10.
(40) Wade, J. L.; Bergold, A. F.; Carr, P. W. Theoretical description of nonlinear chromatography, with applications to psychochemical measurements in affinity chromatography and implications for preparative-scale separations. *Anal. Chem.* **1987**, *59*, 1286−1295.
(41) *PeakFit for Windows*, version 4.11; SPSS Inc.: Chicago, IL, 2001.
(42) *Cerius2*, version 4.8; Accelrys Inc.: San Diego, CA, 2000.
(43) *HyperChem*, version 6.0; Hypercube Inc.: Gainesville, FL, 2000.
(44) *STATISTICA*, version 6.0: Statsoft Inc.: Tulsa, OK, 2001.
(45) Oiki, S.; Danho, W.; Madison, V.; Montal, M. M2 delta, a candidate for the structure lining the ionic channel of the nicotinic cholinergic receptor. *Proc. Natl Acad. Sci. U.S.A.* **1988**, *85*, 8703−8707.
(46) Montal, M. Molecular mimicry in channel−protein structure. *Curr. Opin. Struct. Biol.* **1995**, *5*, 501−506.
(47) Marsh, D. Peptide models for membrane channels. *Biochem. J.* **1996**, *315*, 345−361.
(48) Opella, S. J.; Marassi, F. M.; Gesell, J. J.; Valente, A. P.; Kim, Y.; Oblatt-Montal, M.; Montal, M. Structures of the M2 channel-lining segments from nicotinic acetylcholine and NMDA receptors by NMR spectroscopy. *Nat. Struct. Biol.* **1999**, *6*, 374−379.
(49) *SYBYL*, version 6.8; Tripos Inc., St. Louis, MO, 2002.
(50) Pearlman, D. A.; Case, D. A.; Caldwell, J. W.; Ross, W. S.; Cheatham, T. E., III; DeBolt, S.; Ferguson, D.; Seibel, G.; Kollman, P. AMBER, a package of computer programs for applying molecular mechanics, normal mode analysis, molecular dynamics and free energy calculations to simulate the structural and energetic properties of molecules. *Comput. Phys. Commun.* **1995**, *91*, 1−41.
(51) Cornell, W. D.; Cieplak, P.; Bayly, C. I.; Gould, I. R.; Merz, K. M., Jr.; Ferguson, D. M.; Spellmeyer, D. C.; Fox, T.; Caldwell, J. W.; Kollman, P. A. A second generation force field for the simulation of proteins, nucleic acids, and organic molecules *J. Am. Chem. Soc.* **1995**, *117*, 5179−5197.
(52) Laskowski, R. A.; MacArthur, M. W.; Moss, D. S.; Thornton, J. M. PROCHECK: a program to check the stereochemical quality of protein structures. *J. Appl. Crystallogr.* **1993**, *26*, 283−291.

(53) Stewart, J. J. P. Semiempirical molecular orbital methods. In *Reviews in Computational Chemistry*; Lipkowitz, K. B., Boyd, D. B., Eds.; VCH: New York, 1990; Vol. 1, pp 45−81.
(54) Morris, G. M.; Goodsell, D. S.; Halliday, R. S.; Huey, R.; Hart, W. E.; Belew, R. K.; Olson, A. J. Automated docking using a lamarckian genetic algorithm and an empirical binding free energy function. *J. Comput. Chem.* **1998** *19*, 1639−1662.
(55) Goodsell, D. S.; Morris, G. M.; Olson, A. J. Docking of flexible ligands: applications of AutoDock. *J. Mol. Recognit.* **1996**, *9*, 1−5.
(56) Mehler, E. L.; Solmajer, T. Electrostatic effects in proteins: comparison of dielectric and charge models. *Protein Eng.* **1991**, *4*, 903−910.
(57) Sanner, M. F.; Spehner, J.-C.; Olson, A. J. Reduced Surface: an efficient way to compute molecular surfaces. *Biopolymers* **1996**, *38*, 305−320.
(58) Lee, I. S.; Park, T. J.; Suh, B. C.; Kim, Y. S.; Rhee, I. J.; Kim, K. T. Chlorpromazine-induced inhibition of catecholamine secretion by a differential blockade of nicotinic receptors and L-type Ca^{2+} channels in rat pheochromocytoma cells. *Biochem. Pharmacol.* **1999**, *58*, 1017−1024.
(59) Yu, Y.; Shi, L.; Karlin, A. Structural effects of quinacrine binding in the open channel of the acetylcholine receptor. *Proc. Natl. Acad. Sci. U.S.A.* **2003**, *100*, 3907−3912.
(60) Arias, H. R. The high-affinity quinacrine binding site is located at a non-annular lipid domain of the nicotinic acetylcholine receptor. *Biochim. Biophys. Acta* **1997**, *1347*, 9−22.
(61) Kaliszan, R.; Wainer, I. W. Combination of biochromatography and chemometrics: a potential new research strategy in molecular pharmacology and drug design. In *Chromatographic Separations Based on Molecular Recognition*; Jinno, K., Ed.; Wiley-VCH: New York, 1997; pp 273−302.
(62) Okamoto, Y.; Yashima, E. Chromatographic enantiomer separation on chiral polymers. In *Chromatographic Separations Based on Molecular Recognition*; Jinno, K., Ed.; Wiley-VCH: New York, 1997; pp 239−272.

JM0400707